Automotive Applications of Contactless Heart Rate Measurement System Using FMCW Radar and LSTM

1st Asma Omri
COSIM Lab
SUP'COM, University of Carthage
Innovation Department
ACTIA Engineering Services
Ariana, Tunisia
asma.omri@supcom.tn

2nd Iheb Sifaoui
Innovation Department
ACTIA Engineering Services
Ariana, Tunisia
iheb.sifaoui@actia-engineering.tn

3rd Mohamed Kaouech
SUP'COM, University of Carthage
Ariana, Tunisia
mohamed.kaouech@supcom.tn

4th Sofiane Sayahi
Innovation Department
ACTIA Engineering Services
Ariana, Tunisia
sofiane.sayahi@actia-engineering.tn

5th Hichem Besbes
COSIM Lab
SUP'COM, University of Carthage
Ariana, Tunisia
hichem.besbes@supcom.tn

***Abstract*—In this paper, we propose a system that utilizes the AWR6843AOP radar from Texas Instruments to extract precise vital sign information, particularly focusing on drowsiness detection for future autonomous systems. The radar allows us to estimate Ballistocardiogram (BCG) signals, which capture the mechanical movements of the body, making them suitable for heart rate estimation. We address the challenges associated with FMCW radar-based vital sign monitoring by implementing Long Short-Term Memory (LSTM) networks, which outperform traditional signal processing techniques. A comprehensive data collection system was established for dataset construction and LSTM training, and the heart rate estimation through LSTM delivers an average accuracy of approximately 91% with an RMSE of 1.01 beat per minute (bpm). The system was evaluated with twenty participants in various scenarios, showing promising results for continuous monitoring applications in real-world conditions, including within a moving vehicle equipped with the radar system.**

***Index Terms*—Ballistocardiogram, FMCW Radar, vital sign monitoring, LSTM**

I. Introduction

Autonomous vehicles of nowadays include a high number of assistance systems to enhance driver safety. Radar system have been widely used to monitor the condition of the driver in a car wince they can provide non-intrusive Ballistocardiogram (BCG) measurement. BCG is a cardiac vibration signal that has been widely studied for continuous monitoring of heart rate. The importance of heart rate estimation in cars lies in its potential to increase driver safety detect signs of fatigue, stress or other health conditions that may affect the driver's ability. Many studies have been conducted to measure the human heart rate accurately using FMCW radar. The paper in [1] proposes a novel algorithm for instantaneous heartbeat detection using a 24 GHz continuous wave (CW) radar system using a technique based on template matching of the cross-correlation. The results are encouraging, but the performances went down for a moving subject. The authors in [2] introduced the "coarse to fine" method for more accurate human heart rate extraction using mmWave radar. It uses an adaptive threshold to filter out erroneous peaks from the phase signal, then estimates both heart and breathing rates with spectral domain analysis. The method in [3] increased accuracy by removing invalid peak–valley pairs and adjusting the observation window in order to reduce heartbeat harmonics caused by respiration. Also, in [4], the location and BCG signals of three people could be discriminated simultaneously in one room using the phase-tracking method of the multiple-input–multiple-output (MIMO) FMCW signal. HR and BR monitoring for several patients at once was proposed in [5] by using frequency modulated continuous wave (FMCW) mmWave radar. A new method is presented that combines several processing techniques using a least squares solution to improve measurement precision, generalization, and handling of errors. The proposed approach optimized the observation window size for vital sign detection by considering peak difference [6]. A novel method using a 77 GHz FMCW radar sensor was proposed in [7] to extract respiration and heart rate in an indoor environment, addressing the challenge of interference and achieving high results compared to a reliable smart bracelet. FMCW radars with various carrier frequencies—24 GHz, 60 GHz, and 120 GHz—are the subject of [8]. Assessments of baseline noise, range estimation error,

and displacement estimation error are conducted on human subjects and phantom models. The authors of [9] presented a sampling theory based method in which the frame structure of recent FMCW radars is obtained by adding extra chirp repetition within each frame. The heartbeat signal can be sampled faster or slower than 50ms period. In [10], the authors proposed a real-time drowsiness detection system using a 77 GHz FMCW radar based on Drowsiness classification model using extreme gradient boosting algorithms.

A deep learning (DL)-aided weighted system was proposed in [11] for implementing a vital sign system for fast acquisition and accurate estimation especially during epidemic outbreaks. The system fuses observations to reduce the required size of the observation signal, enabling fast acquisition, and employs a convolutional neural network (CNN) for accurate vital sign detection. The system acheived satisfactory performance with limited observations for fast acquisition. The absolute error of 90% breathing measurements is less than 3 respirations per minute (rpm), and the absolute error of 75% heartbeat measurements is less than 3 beats per minute (bpm).

Several approaches based on the use of the Long Short Term Memory (LSTM) [12] networks were proposed to analyze and classify the electrocardiogram (ECG) signals. The paper in [13] presents a novel ECG classification algorithm for continuous heart rate monitoring with wearable devices and limited processing capacity. The proposed solution employs a novel architecture consisting of wavelet transform and multiple LSTM Recurrent Neural Networks RNN and achieves high ECG classification performance compared to previous works. The algorithm satisfy the real-time requirements for execution on wearable devices. The paper [14] proposes a deep learning (DL)-aided weighted scheme for implementing a vital sign system using a dynamically-biased Long Short-Term Memory (DB-LSTM) network.

A deep learning model was proposed in [15] for automatic heartbeat detection from **ballistocardiogram** (BCG) signals based on UNet and bidirectional Long Short-Term Memory (Bi-LSTM). The extracted BCG signal is based on a piezo-electric sensor module and a data processor placed under a pillow of a patient sleeping on a bed with a measurement frequency of 1 kHz. The authors of [16] propose a novel deep learning model for automatic heartbeat detection from BCG signals. The BCG signal is extracted using Optical Fiber Sensor (OFS). The model combines a Convolutional Neural Network (CNN) for short-term dependence extraction, a recurrent neural network (RNN) for long-term dependence capture, and an LSTM with a recurrent skip for ultra-long-term repetitive pattern analysis.

In this paper, we present an approach inspired by prior works by [15] and [17] , where the BCG signal is acquired using an FMCW radar technology. Specifically, our study focuses on monitoring the BCG signal of a driver within a moving vehicle. This introduces several unique challenges compared to existing solutions. The paper is organized as follows: Section II presents the system model. Section III presents the heart rate estimation based on the LSTM approach. Section IV explains the adopted methodology to build a dataset for the LSTM training. Section V discusses the obtained results. The conclusion is presented in section VI.

II. System Model

A. FMCW Radar

The FMCW radar transmits a frequency modulated signal (chirp) given by equation (1) whose frequency increases linearly with time:

$$s_T(t) = \exp\left(i2\pi f_c t\right) \exp\left(i\pi\beta t^2\right) \quad where \quad \beta = \frac{B}{T} \tag{1}$$

where f_c, B, T and β are the carrier frequency, the signal's bandwidth, the signal's period and the sweep slope.

Assume that the transmitted signal hits L objects. Each object n is at a range r_n from the radar, the returned signal is expressed by equation (2), as follows:

$$y(t) = \sum_{n=1}^{L} \alpha_n s_T(t - \tau_n) \tag{2}$$

Where τ_n is a round trip delay given by $\tau_n = \frac{2R_n}{c}$and α_n is the attenuation of the path n.

The received signal is mixed with the transmitted signal to obtain the Intermediate Frequency IF signal given by equation (3). The IF signal is proportional to the beat frequency, which is the difference between the transmitted and received frequencies. It used to estimate the target's path parameters, such as its range, velocity, and direction.

$$z(t) = \sum_{n=1}^{L} \alpha_n^* \exp\left(i2\pi f_c \frac{2R_n}{c}\right) \exp\left(-i\pi\beta\left(\frac{2R_n}{c}\right)^2\right) \exp\left(i2\pi\beta\left(\frac{2R_n}{c}\right)t\right) \tag{3}$$

To estimate the range R_n, one may estimate the beat frequencies $f_{b,n}$ given by:

$$f_{b,n} = \beta\left(\frac{2R_n}{c}\right) \tag{4}$$

by sampling the IF signal and apply a simple FFT. For more information about FMCW radar, the interested reader can refer to [18].

B. Chest Wall Motion

Ballistocardiography is a non-invasive medical technique that involves recording the oscillations of the human body caused by the movement of blood in the circulatory system. It makes it possible to analyze cardiac and vascular dynamics, in particular the resistance of the aorta. BCG [19] is a cardiac vibration signal that has been widely studied for continuous monitoring of heart rate. Conventional methods in BCG signals necessitates the use of specialized equipment as well as its correct placement. The sensor has to come into touch with the body. Further analysis needs to be done to extract the peaks relative to the hearbeats.

In this work, we measure the BCG signal by measuring the chest wall displacement by placing an FMCW radar in front of the subject as depiucted in figure 1

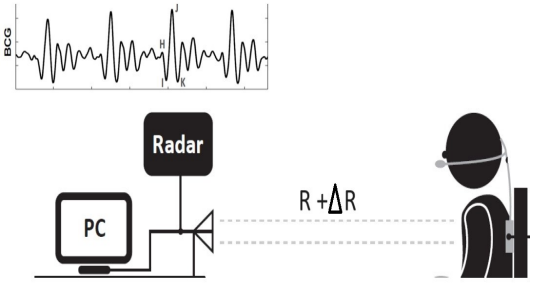

Fig. 1: Example of BCG waveforms acquired by a modified weighing scale [19].

The chest wall motion comprises two components: the displacement from respiration activity and the displacement due to cardiac activity. A mathematical model addresses this, considering heart-induced motion (typically 0.2–0.5 mm) and its time-varying pulse, aiming to tackle the complexities of cardiorespiratory activity [20]. Both cardiac activity and respiration contribute to the displacement of the chest wall during normal breathing. However, only heart activity causes a very little amount of displacement in comparison to respiration-induced displacement during breath retention. The displacement of the chest wall ranges from 4 to 12 mm, which is equivalent to variations in the peak amplitude parameter of 0.035 to 0.11 [20]. The chest displacement seen from the radar can be modeled as follows:

$$\begin{aligned} R(t) = &\quad R + \Delta R(t) \\ R(t) = &\quad R + g_{br}(t, f_{br}) + g_{hr}(t, f_{hr}) + g_{bh}(t, f_{br}, f_{hr}) \end{aligned} \tag{5}$$

Where R is the distance from the radar and the chest, $\Delta R(t)$ is the micro-displacement of the chest, f_{br} and f_{hr} are the breath respiratory and heartbeat frequencies, $g_{br}(t, f_{br})$ and $g_{hr}(t, f_{hr})$ are two periodic functions with frequencies f_{br} and f_{hr} modeling the chest movement, and $g_{bh}(t, f_{br}, f_{hr})$ models the inter-modulation between the movements due to respiratory and heartbeat.

C. Heart Rate measurement

At the radar, the beat signal $b(t)$ from an object at range R after mixing and filtering is given by 6. The change in phase of the beat signal $\Delta\phi_b$ with time when the target moves a distance ΔR is measured to identify the small displacement in the chest as given by equations 6 and 7:

$$\begin{aligned} b(t) = &\quad exp\left(i\left(4\pi\frac{BR}{cT_c}t + \frac{4\pi}{\lambda}\Delta R\right)\right) \\ b(t) = &\quad exp\left(i\left(2.\pi f_b t + \phi_b\right)\right) \end{aligned} \tag{6}$$

where λ, f_b and ϕ_b are the wavelength, the beat frequency and the phase of the beat signal.

$$\Delta\phi_b = \frac{4\pi}{\lambda}\Delta R \tag{7}$$

When we perform the FFT and the object is at range-bin m, the vibration signal $x(t)$, given by equation 8, can be obtained by measuring the phase at range-bin m at time indices nTs, where n is the chirp index and Ts is the interval between successive measurements. The range bin indicates the position of the individual being tracked.

$$x\left(m, nT_s\right) = \frac{\lambda}{4\pi}\phi_b\left(m, nT_s\right) \tag{8}$$

In the phase signal we capture the chest displacement modeled in equation 5. One approach to estimate the heart and respiration rates is described in figure 2. The radar signal's phase is extracted from the range bin obtained from the range FFT. The extracted phase is preserved in a sliding window arrangement. This selection is updated every few seconds depending on the frame rate of the radar which is 50 ms in most of the cases. The extracted phase is then unwrapped. Phase unwrapping is a process used to eliminate discontinuities in the phase signal, which typically occur when the phase value jumps between $-\pi$ and π. The system calculates phase differences, which is a step that involves taking the difference between consecutive phase values to detect changes over time.

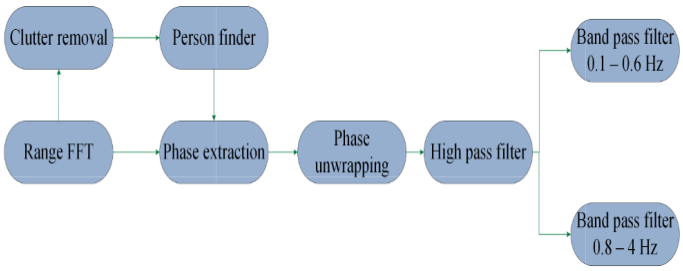

Fig. 2: Heart rate and breathing rate estimation diagram.

The unwrapped phase signal is divided into two distinct waveforms: heart waveform and breathing waveform. Furthermore, it passed through two bandpass filters: the first with a bandpass of 0.1 to 0.5 Hz, which keeps the breathing waveform, the second with a bandpass of 0.8 to 4 Hz, which keeps the heart waveform. The cut off frequencies represent the maximum and minimum heart rate and breathing desired. A circular buffer holds the data from these two different waveforms. This buffer functions similarly to a sliding window. A typical BCG signal measured by the FMCW radar is depicted in the figure 3:
The heart rate estimation can be approximated using spectral estimation techniques including Fast Fourier Transform (FFT). The major drawback of these techniques, is the appearance of the inter-modulation between the heartbeat and breath rate, which may lead to low performance system.

To overcome this challenge, we propose in this paper to use an LSTM network to estimate the heart rate from the measured BCG signal.

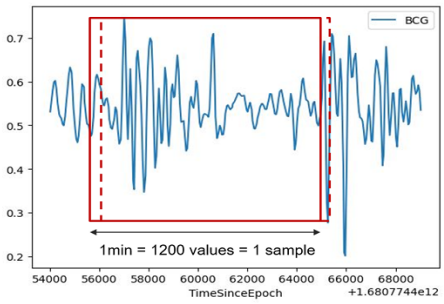

Fig. 3: BCG Signal Measured by the FMCW Radar

III. Vital Sign Estimation based on LSTM approach

Accurate heart rate estimate with conventional mmWave radars usually requires a static measurement environment. Heart rate estimate errors can arise in dynamic setups like moving radars due to the continuous changes in the surrounding environment. To address this problem, Long Short-Term Memory (LSTM) networks have been used to improve the accuracy of heart rate estimation in dynamic environments by accounting the temporal dependencies in the data.

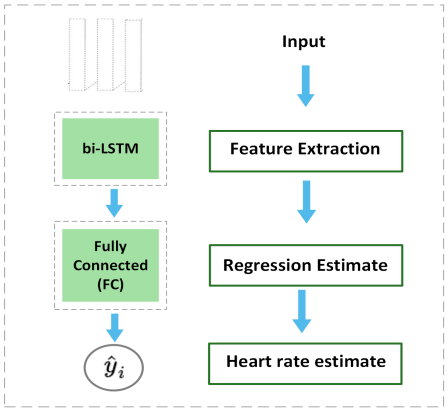

Fig. 4: LSTM architecture.

We modeled heart rate estimation as a regression problem from BCG signals. We developed a deep learning network to extract cross-correlation features and integrate them into a regression block to predict heart rates as shown in the architecture of our model in Figure 4. The BCG data was browsed through a sliding window of one minute with a step length of 1s. In practice, we have set the window length at 1200 values and sliding step at 20 values. The data in the corresponding sliding window were taken as training sample. Extracting heartbeat features from BCG segments is carried out using a using a bi-directional Long Short-Term Memory bi-LSTM network as shown in Figure 4.

In opposition to a standard LSTM network, a bi-LSTM aids in resolving issues related to gradient expansion and disappearance during long sequence training. A dense two-layer network Fully connected (FC) is designed for the regression estimate to make a correspondence between the bi-LSTM features and the actual heart rate values as shown in Figure 5. The extracted features coming out of the bi-LSTM network are rescaled into a one-dimensional vector before passing to the dense layers. Designing such a network not only allows efficient convergence during training, but also avoids the disappearance of the gradient in the network flow.

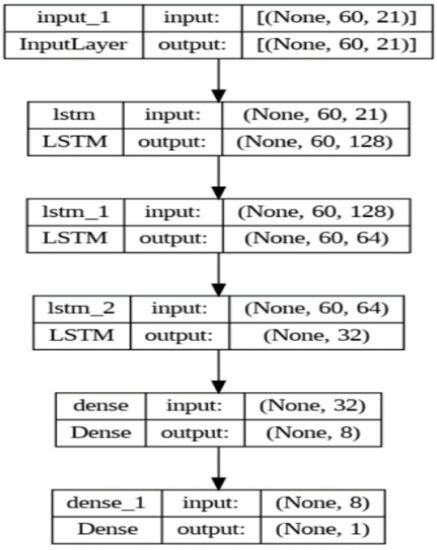

Fig. 5: LSTM layers.

IV. Dataset Creation

A. Dataset Description

To evaluate the performance of our proposed architecture, we have developed an acquisition system composed of three main sensors:

- The AWR6843AOP radar: is a single-chip mmWave sensor with the Antenna-on-Package (AOP) technology developed by Texas Instruments and designed for vital signs monitoring.
- The Suunto cardio belt: is a chest belt connected to an application installed on the phone via Bluetooth.
- Garmin watch: connected to an application installed on the phone via Bluetooth.
- Oxymeter: connected to an application installed on the phone via Bluetooth.

The chest belt and the watch are used as two references for the heart rate estimation. The collected dataset comprises overall 3 hours of recording measurement of the BCG signal from the radar along with the heart rates from the others sensors. For each sample the value of BCG signal as well as the associated nanosecond timestamp were recorded. The dataset is acquired for different setups mainly static and dynamic and for 10 persons. Measuring in a dynamic environment is a crucial aspect for vital signs monitoring since it is closer to the real-world scenarios for automotive applications. These tests are performed with a moving car.

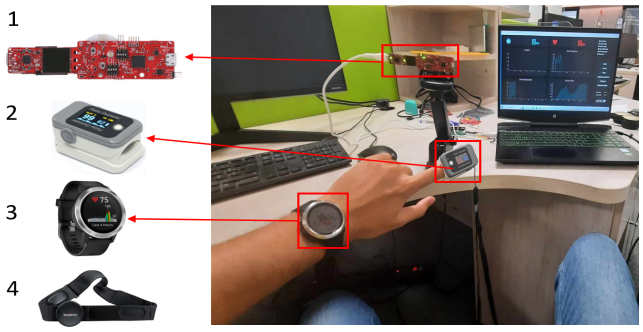

Fig. 6: Data acquisition system setup for static scenarios.

(a) (b)

Fig. 7: Data acquisition system setup for dynamic scenarios.

B. Sensors Synchronization

Since the sensors used in the data acquisition system are operating in different frequencies, the synchronization of the data is crucial for temporal alignment and comprehensive performance evaluation of the proposed architecture. We have used the synchronization with timestamps which involves associating a time value with each BCG signal, enabling the temporal alignment of information from the three sensors.

C. Data Processing

To monitor heart rate variations in real time, we have chosen to estimate the heart rate every second over the past minute. The BCG data is processed using a 1-minute sliding window with a 1-second step length. The window is set to 1200 values, and the sliding step is set to 20 values. The data within the sliding window is then used as the training sample.

V. Experimental Results

A. Hyper-parameter Tuning

Defining the training configuration is as important as defining the architecture of our model. The key elements are the cost function we want to minimize and the optimizer used during training, as well as the techniques used to regularize the weights and avoid overfitting. We used Mean Square Error MSE, and the Root MSE given in equations 9 and 10 to measure the performance of our model.

$$\text{MSE} = \frac{1}{n}\sum_{i=1}^{n}\left(Y_i - \hat{Y}_i\right)^2 \tag{9}$$

$$RMSE = \sqrt{MSE} = \sqrt{\frac{1}{N}\sum_{i=1}^{N}(y_i - \hat{y})^2} \tag{10}$$

We chose the Adam optimization algorithm, which is a stochastic gradient descent method. The Adam optimizer is used with its default configuration and with a learning rate (LR) initially set to LR= 0.0001.

B. performance Evaluation

When assessing the performance of a machine learning model during training it is important to examine both the training loss and validation loss curves. These curves illustrate how the loss decreases over epochs as the model learns from the training data as shown by the Training Loss curve. As training progresses the high loss gradually converges towards a value. On the hand the Validation Loss curve showcases how well the model performs on a dataset indicating its ability to generalize. Ideally we would want to see a starting point, for validation loss; however it might increase if the model becomes too focused, on fitting to the training data.

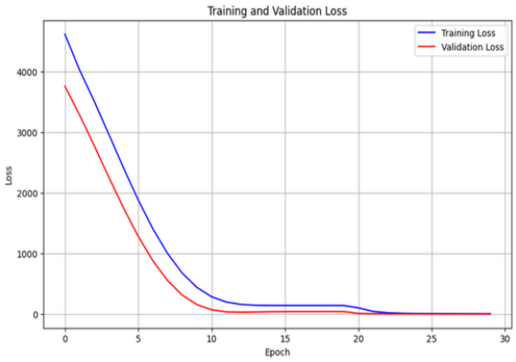

Fig. 8: Training and validation loss curves.

The results we obtained show a Root Mean Square Error (RMSE) of 1.015 for the test data. To be more precise, this means that on average our predictions differ by about 1,015 units from the actual values. A lower RMSE is generally associated with better model accuracy, which suggests that our model fits the test data quite accurately.

Conclusion

In this paper, we have proposed a system composed of an FMCW radar aiming to precisely estimate the heart rate in conjunction with an LSTM network for drowsiness detection. The performance of the network is evaluated with a comprehensive dataset collected from the AWR6843AOP TI radar with a reference to a chest belt and a watch providing the ground truth of heart rate. The system has been proven to be precise and robust given the variety of data acquisition system setups in static and dynamic environment. Our system

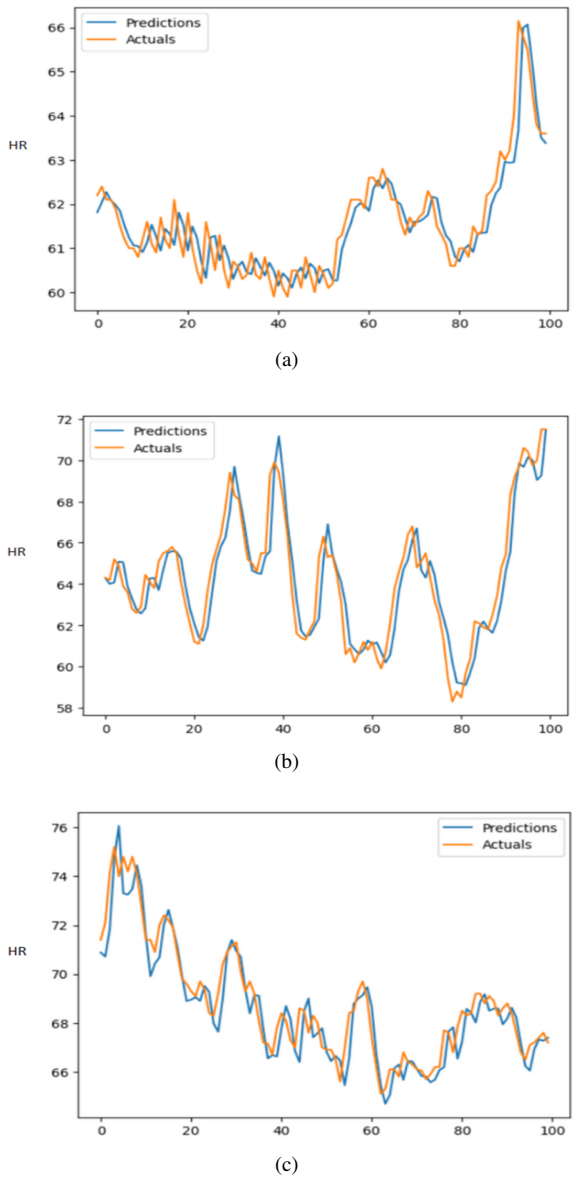

Fig. 9: Data acquisition system setup for dynamic scenarios.

outperform the conventional methods of heart estimation with an overall accuracy of 91 % and an RMSE of 1.01 beat per minute (bpm). This system not only improves safety of drivers on the roads but also paves the way for its integration into the automotive ecosystem to enhance driver well-being.

REFERENCES

[1] C. Will, K. Shi, F. Lurz, R. Weigel, and A. Koelpin, "Instantaneous heartbeat detection using a cross-correlation based template matching for continuous wave radar systems," in *2016 IEEE Topical Conference on Wireless Sensors and Sensor Networks (WiSNet)*, Jan 2016, pp. 31–34.

[2] K. Liu, C. Ding, and Y. Zhang, "A coarse-to-fine robust estimation of fmcw radar signal for vital sign detection," in *2020 IEEE Radar Conference (RadarConf20)*, Sep. 2020, pp. 1–6.

[3] M. Zhou, Y. Liu, S. Wu, C. Wang, Z. Chen, and H. Li, "A novel scheme of high-precision heart rate detection with a mm-wave fmcw radar," *IEEE Access*, vol. 11, pp. 85 118–85 136, 2023.

[4] K. Han and S. Hong, "Detecting locations and vital signs of multiple humans with mimo fmcw radar," in *2021 International Symposium on Antennas and Propagation (ISAP)*, 2021, pp. 1–2.

[5] J. Benny, P. Mahajan, S. S. Chatterjee, M. Wajid, and A. Srivastava, "Design and measurements of mmwave fmcw radar based non-contact multi-patient heart rate and breath rate monitoring system," in *2023 IEEE Biomedical Circuits and Systems Conference (BioCAS)*, Oct 2023, pp. 1–5.

[6] W. A. Ahmad, J.-H. Lu, B. Sutbas, H. J. Ng, and D. Kissinger, "Contactless vital signs monitoring by mmwave efficient modulatorless tracking radar," in *2021 IEEE Global Conference on Artificial Intelligence and Internet of Things (GCAIoT)*, Dec 2021, pp. 142–146.

[7] M. Xiang, W. Ren, W. Li, Z. Xue, and X. Jiang, "High-precision vital signs monitoring method using a fmcw millimeter-wave sensor," *Sensors*, vol. 22, no. 19, 2022. [Online]. Available: https://www.mdpi.com/1424-8220/22/19/7543

[8] S. Marty, F. Pantanella, A. Ronco, K. Dheman, and M. Magno, "Investigation of mmwave radar technology for non-contact vital sign monitoring," in *2023 IEEE International Symposium on Medical Measurements and Applications (MeMeA)*, June 2023, pp. 1–6.

[9] D. Jung, S. Cheon, D. Kim, J. Yoon, and B. Kim, "Short-time remote heart rate measurement based on mmwave fmcw radar frame structure," *IEEE Antennas and Wireless Propagation Letters*, vol. 22, no. 6, pp. 1301–1305, 2023.

[10] S. Liu, L. Zhao, X. Yang, Y. Du, M. Li, X. Zhu, and Z. Dai, "Remote drowsiness detection based on the mmwave fmcw radar," *IEEE Sensors Journal*, vol. 22, no. 15, pp. 15 222–15 234, Aug 2022.

[11] H.-Y. Chang, C.-H. Hsu, and W.-H. Chung, "Fast acquisition and accurate vital sign estimation with deep learning-aided weighted scheme using fmcw radar," in *2022 IEEE 95th Vehicular Technology Conference: (VTC2022-Spring)*, June 2022, pp. 1–6.

[12] L. S.-T. Memory, "Long short-term memory," *Neural computation*, vol. 9, no. 8, pp. 1735–1780, 2010.

[13] S. Saadatnejad, M. Oveisi, and M. Hashemi, "Lstm-based ecg classification for continuous monitoring on personal wearable devices," *IEEE Journal of Biomedical and Health Informatics*, vol. 24, no. 2, pp. 515–523, Feb 2020.

[14] J. Hu, W. L. Goh, and Y. Gao, "Classification of ecg anomaly with dynamically-biased lstm for continuous cardiac monitoring," in *2023 IEEE International Symposium on Circuits and Systems (ISCAS)*, May 2023, pp. 1–5.

[15] Y. Mai, Z. Chen, B. Yu, Y. Li, Z. Pang, and Z. Han, "Non-contact heartbeat detection based on ballistocardiogram using unet and bidirectional long short-term memory," *IEEE Journal of Biomedical and Health Informatics*, vol. 26, no. 8, pp. 3720–3730, Aug 2022.

[16] Q. Wang, W. Lyu, S. Chen, and C. Yu, "Noninvasive human ballistocardiography assessment based on deep learning," *IEEE Sensors Journal*, vol. 23, no. 12, pp. 13 702–13 710, June 2023.

[17] C. Jiao, C. Chen, S. Gou, D. Hai, B.-Y. Su, M. Skubic, L. Jiao, A. Zare, and K. C. Ho, "Non-invasive heart rate estimation from ballistocardiograms using bidirectional lstm regression," *IEEE Journal of Biomedical and Health Informatics*, vol. 25, no. 9, pp. 3396–3407, Sep. 2021.

[18] S. Pisa, E. Pittella, and E. Piuzzi, "A survey of radar systems for medical applications," *IEEE Aerospace and Electronic Systems Magazine*, vol. 31, no. 11, pp. 64–81, November 2016.

[19] L. Giovangrandi, O. T. Inan, R. M. Wiard, M. Etemadi, and G. T. Kovacs, "Ballistocardiography — a method worth revisiting," in *2011 Annual International Conference of the IEEE Engineering in Medicine and Biology Society*, Aug 2011, pp. 4279–4282.

[20] A. Singh, S. U. Rehman, S. Yongchareon, and P. H. J. Chong, "Modelling of chest wall motion for cardiorespiratory activity for radar-based ncvs systems," *Sensors*, vol. 20, no. 18, p. 5094, 2020.